0026-895X/07/7206-1637–1646
MOLECULAR PHARMACOLOGY
U.S. Government work not protected by U.S. copyright
Mol Pharmacol 72:1637–1646, 2007

Vol. 72, No. 6
39644/3278788
Printed in U.S.A.

Cystine-Glutamate Transporter SLC7A11 Mediates Resistance to Geldanamycin but Not to 17-(Allylamino)-17-demethoxygeldanamycin[S]

Ruqing Liu, Paul E. Blower, Anh-Nhan Pham, Jialong Fang, Zunyan Dai, Carolyn Wise, Bridgette Green, Candee H. Teitel, Baitang Ning, Wenhua Ling, Beverly D. Lyn-Cook, Fred F. Kadlubar, Wolfgang Sadée, and Ying Huang

Division of Pharmacogenomics and Molecular Epidemiology (R.L., C.W., B.G., C.H.T., B.N., B.D.L.-C., Y.H.), and Division of Biochemical Toxicology (J.F.), National Center for Toxicological Research, Food and Drug Administration, Jefferson, Arkansas; School of Public Health, Sun Yat-sen University, Guangzhou, China (R.L., W.L.); Program of Pharmacogenomics, Department of Pharmacology, Comprehensive Cancer Center, College of Medicine and Public Health, the Ohio State University, Columbus, Ohio (P.E.B., Z.D., W.S.); Department of Epidemiology, University of Arkansas for Medical Sciences, Little Rock, Arkansas (F.F.K.); Department of Pharmaceutical Sciences, College of Pharmacy, Western University of Health Sciences, Pomona, California (A.-N.P., Y.H.)

Received July 9, 2007; accepted September 17, 2007

ABSTRACT

The cystine-glutamate transporter SLC7A11 has been implicated in chemoresistance, by supplying cystine to the cell for glutathione maintenance. In the NCI-60 cell panel, SLC7A11 expression shows negative correlation with growth inhibitory potency of geldanamycin but not with its analog 17-(allylamino)-17-demethoxygeldanamycin (17-AAG), which differs in the C-17 substituent in that the the methoxy moiety of geldanamycin is replaced by an amino group. Structure and potency analysis classified 18 geldanamycin analogs into two subgroups, "17-O/H" (C-17 methoxy or unsubstituted) and "17-N" (C-17 amino), showing distinct SLC7A11 correlation. We used three 17-O/H analogs and four 17-N analogs to test the role of the 17-substituents in susceptibility to SLC7A11-mediated resistance. In A549 cells, which are resistant to geldanamycin and strongly express SLC7A11, inhibition of SLC7A11 by (*S*)-4-carboxyphenylglycine or small interfering RNA increased sensitivity to 17-O/H, but had no effect on 17-N analogs. Ectopic expression of SLC7A11 in HepG2 cells, which are sensitive to geldanamycin and express low SLC7A11, confers resistance to geldanamycin, but not to 17-AAG. Antioxidant *N*-acetylcysteine, a precursor for glutathione synthesis, completely suppressed cytotoxic effects of 17-O/H but had no effect on 17-N analogs, whereas the prooxidant ascorbic acid had the opposite effect. Compared with 17-AAG, geldanamycin led to significantly more intracellular reactive oxygen species (ROS) production, which was quenched by addition of *N*-acetylcysteine. We conclude that SLC7A11 confers resistance selectively to 17-O/H (e.g., geldanamycin) but not to 17-N (e.g., 17-AAG) analogs partly as a result of differential dependence on ROS for cytotoxicity. Distinct mechanisms could significantly affect antitumor response and organ toxicity of these compounds in vivo.

Chemoresistance is a major cause of treatment failure in patients with cancer. Multiple mechanisms may contribute to resistance to chemotherapy, including alterations of drug transport and metabolism, drug target, DNA repair, cell proliferation and death (Huang and Sadee, 2003). A systematic approach in screening anticancer drugs is needed for identifying drug candidates among a series of congeners to avoid chemoresistance. We have developed a method to study the potential pharmacological interactions between transporter proteins and anticancer drugs (Huang et al., 2004). We applied a custom-designed microarray to analyze gene expression of a majority of human membrane transporters and ion

This work was supported in part by National Institutes of Health research grant GM61390 from National Institute of General Medical Sciences and by the U.S. Food and Drug Administration.

The views presented in this article do not necessarily reflect those of the US Food and Drug Administration.

Article, publication date, and citation information can be found at http://molpharm.aspetjournals.org.

doi:10.1124/mol.107.039644.

[S] The online version of this article (available at http://molpharm.aspetjournals.org) contains supplemental material.

ABBREVIATIONS: DTP, Developmental Therapeutics Program; NCI, National Cancer Institute; ROS, reactive oxygen species; GA, geldanamycin; 17-AAG, 17-(allylamino)-17-demethoxygeldanamycin; Hsp90, 90-kDa heat shock protein; 17-DMAG, 17-(2-dimethylaminoethyl)amino-17-demethoxygeldanamycin; SRB, sulforhodamine B; 4-*S*-CPG, (*S*)-4-carboxyphenylglycine; 17-AEP-GA, 17-(2-(pyrrolidin-1-yl)ethyl)amino-17-demethoxygeldanamycin; 17-DMAP-GA, 17-(dimethylaminopropylamino)-17-demethoxygeldanamycin; NAC, *N*-acetylcysteine; AsA, ascorbic acid; H_2DCFDA, dichlorodihydrofluorescein diacetate; PBS, phosphate-buffered saline; MOA, mechanism of action; PCA, principal component analysis; siRNA, small interfering RNA; RT-PCR, reverse transcription-polymerase chain reaction.

channels (namely, the transportome) in the NCI-60 cell panel, which is used by the Developmental Therapeutics Program (DTP) of the National Cancer Institute (NCI) for anticancer drug screening. Correlating gene expression levels with the growth inhibitory potencies of anticancer drugs in the NCI-60 cells, we have identified known drug-transporter interactions and suggested novel ones (Huang et al., 2004; Huang et al., 2005a; Dai et al., 2006). For a given gene-drug pair, high expression of a given gene in drug-sensitive cell lines yields positive correlation coefficients, whereas high expression in resistant cells gives negative correlation coefficients. Expanding this methodology, we also developed data mining techniques for identifying structural features of compounds showing activity patterns highly correlated with specific mRNA expression patterns (Blower et al., 2002). The approach was used to discover novel associations between compound classes and drug transporters (Huang et al., 2005b; Dai et al., 2007).

SLC7A11 (or xCT), together with SLC3A2 (or 4F2hc), encodes the heterodimeric amino acid transport system x_c^-, which mediates entry of cystine into the cell coupling to efflux of glutamate (Sato et al., 2000). SLC7A11, the light chain of system x_c^-, is thought to mediate the transport activity, whereas SLC3A2, the heavy chain, leads to the surface expression of the system x_c^- (Verrey et al., 2004). Once inside the cell, cystine is rapidly reduced to cysteine, the rate limiting amino acid for GSH biosynthesis (Gatti and Zunino, 2005). In tumor cells, the amino acid transport system x_c^- plays a crucial role in regulating intracellular GSH levels (Okuno et al., 2003). GSH has been broadly implicated in resistance to chemotherapy (Gatti and Zunino, 2005). Driven by a reactive sulfhydryl group, GSH conjugation is a major detoxification pathway (Yang et al., 2006). Many xenobiotics are susceptible to GSH conjugation and detoxification. In addition, GSH protects against cellular damage caused by free radicals and other reactive oxygen species (ROS) such as superoxides and H_2O_2 (Wu et al., 2004). In a previous study (Huang et al., 2005a), SLC7A11 expression in the NCI-60 negatively correlated with activity of multiple anticancer drugs. The number of significant SLC7A11-drug correlations was much greater than those of other genes tested, suggesting that SLC7A11 plays a critical role in chemoresistance. The expression levels of SLC7A11 showed strongest correlation with the activity of geldanamycin (GA; NSC 122750), whereas no correlation was observed with the GA analog 17-(allylamino)-17-demethoxygeldanamycin (17-AAG; NSC 330507) (Huang et al., 2005a). This indicates that structural changes can abolish SLC7A11-mediated chemoresistance, because the only difference between 17-AAG and GA is at the C-17 position.

GA is a benzoquinone ansamycin antibiotic produced by yeast (Whitesell et al., 1994; Smith et al., 2005). Its target is the 90-kDa heat shock protein (Hsp90), an essential protein that maintains stability of "client proteins" implicated in tumor growth and survival, including protein kinases, transcription factors, and mutated oncogenic proteins (Workman, 2004). Treatment of tumor cells with GA results in proteasome-mediated degradation of Hsp90 client proteins. In addition, cytotoxicity of GA on tumors has also been attributed to ROS generation (Dikalov et al., 2002; Lai et al., 2003). Despite potent cytotoxicity on tumors, lethal hepatotoxicity in animals limits the promise of GA as a drug candidate. Synthetic GA analogs have been developed by replacing the C-17 side chains of GA, a potential mediator of liver toxicity (Tian et al., 2004). Two C-17-substituted analogs, 17-AAG and 17-DMAG (17-(2-dimethylaminoethyl)amino-17-demethoxygeldanamycin; NSC 707545), which have reduced liver toxicity but retain cytotoxic potency against tumor cells, have shown encouraging results in clinical trials (Tian et al., 2004).

In the present study, we studied 18 GA analogs to understand the 17-substituent effects of these compounds on their differential susceptibility to SLC7A11-mediated resistance as well as mechanisms of antitumor activity. According to chemical structures and potency across the NCI-60, the 18 compounds can be classified into two distinct groups, "17-O/H" and "17-N," that yield varying correlations with SLC7A11 expression levels. We further showed that SLC7A11 mediates chemoresistance to 17-O/H analogs (e.g., GA), whereas 17-N analogs (e.g., 17-AAG) bypass this resistance mechanism. This study not only improves the understanding of mechanisms for chemoresistance, but also demonstrates the power of our approach to revealing novel drug-transporter relationship and defining structural features associated with SLC7A11-mediated chemoresistance.

Materials and Methods

Compound Potency Databases for NCI-60. The September 2003 release of the National Cancer Institute (NCI) antitumor drug screening database was obtained from the NCI's DTP website (Human Tumor Cell Line Screen: http://dtp.nci.nih.gov/docs/cancer/cancer_data.html), containing nonconfidential screening results and chemical structural data from the DTP. For each compound and cell line, growth inhibition after 48 h of drug treatment was assessed from changes in total cellular protein using a SULFORHODAMINE B (SRB) assay (Weinstein et al., 1997). The data provide GI_{50} values for each compound-cell line pair (GI_{50}, the concentration causing 50% growth inhibition). We clustered the 18 compounds by agglomerative nesting using the complete linkage method (Everitt, 1993; Blower et al., 2004). The compound distance matrix—a measure of similarities or differences in chemical structures—was calculated using the Tanimoto coefficient based on the Leadscope feature set (Leadscope, Columbus, OH) (Blower et al., 2004).

Gene Expression Databases of NCI-60. A customized oligonucleotide microarray containing probes targeting 461 transporter and 151 channel genes, as well as 100 probes for unrelated genes, was used to measure transporter gene expression in NCI-60. Array hybridization, data analysis, and database were described in previous study (Huang et al., 2004). A second gene expression database, the Novartis microarray dataset, was also employed for comparison. This data set contains the average of triplicate expression measurements for 59 NCI cell lines based on 12,626 oligonucleotide probes from Affymetrix U95Av2 arrays, available at NCI's Developmental Therapeutics Program (DTP) web site (http://dtp.nci.nih.gov/mtargets/download.html).

Correlation of Gene Expression Profiles with Compound Potency Patterns. Pearson correlation coefficients were calculated to correlate gene expression profiles with patterns of compound potency across the NCI-60 as described previously (Huang et al., 2005b). Correlation analysis was performed for expression profiles measured with microarrays against the potency of GA analogs. Unadjusted p values were obtained using Efron's bootstrap resampling method (Efron and Tibshirani, 1993), with 10^4 bootstrap samples for each gene-drug comparison.

Principal Component Analysis. PCA was conducted by ArrayTrack version 3.2.0 (NCTR/FDA, AR) (Tong et al., 2003) (http://

www.fda.gov/nctr/science/centers/toxicoinformatics/ArrayTrack/) to explore the relationships of 18 GA analogs based on the potency data (GI_{50}) on NCI-60. PCA maps multidimensional data into a low dimensional graph to visually inspect the drug-drug relationships.

Chemicals. GA, 17-AAG, 17-DMAG, 17-(2-(pyrrolidin-1-yl)ethyl)-amino-17-demethoxygeldanamycin (17-AEP-GA), and 17-(dimethylaminopropylamino)-17-demethoxygeldanamycin (17-DMAP-GA) were purchased from InvivoGen (San Diego, CA). (*S*)-4-Carboxyphenylglycine (4-*S*-CPG) were purchased from Tocris (Ballwin, MO). NSC 658514 and NSC 661581 were obtained from NCI DTP. Others were purchased from Sigma Chemical Co. (St. Louis, MO).

Cell Culture. HepG2 and 293T cells were purchased from the American Type Culture Collection (Manassas, VA) and were cultured in William's Medium E and Dulbecco's modified Eagle's medium, respectively, supplemented with 10% fetal bovine serum, 100 U/ml penicillin G, and 100 μg/ml streptomycin. Other cell lines were obtained from Division of Cancer Treatment and Diagnosis at NCI and cultured in RPMI 1640 medium containing 5 mM L-glutamine, supplemented with 10% fetal bovine serum, 100 U/ml penicillin G, and 100 μg/ml streptomycin. Cells were grown in tissue culture flasks at 37°C in a 5% CO_2 atmosphere.

Cytotoxicity Assay. Growth inhibitory potency was tested using a proliferation assay with SRB, a protein-binding reagent (Sigma), as described previously (Huang et al., 2004). Cells were seeded in 96-well plates (3000–4000/well) and incubated for 24 h. Before exposure to test compounds, cells were treated individually with 4-*S*-CPG, ascorbic acid (AsA, or vitamin C), *N*-acetylcysteine (NAC), or medium (as control) for 10 min. Test compounds were added in a dilution series in three replicated wells for 4 days. To determine IC_{50} values, the absorbance of control cells without drug was set at 1. Dose-response curves were plotted using Prism software (GraphPad Software, San Diego, CA). Each experiment was performed independently at least twice. Student's *t* test was used to determine the degree of significance.

siRNA-Mediated Down-Regulation of SLC7A11. siRNA down-regulation of SLC7A11 expression was described before (Huang et al., 2005a). In brief, siRNA duplexes for SLC7A11 were synthesized using the Silencer siRNA construction kit (Ambion, Austin, TX). The target sequences were 5′-AAATGCCCAGATATGCATCGT-3′, which target nucleotides 1237 to 1257 of the SLC7A11 mRNA sequence NM_014331. Chemically synthesized mock siRNA (fluorescein-labeled, nonsilencing) was purchased from QIAGEN (Valencia, CA). Transfection was performed with HiPerFect Transfection Reagent (QIAGEN) using 5 nM siRNA. To measure cytotoxic drug potency, 24 h after transfection, cells grown in 60-mm plates were subcultured into 96-well plates. After 24 h of incubation, the cells were further incubated with the test compounds for 4 days before cytotoxicity assay.

Cloning and Expression of SLC7A11 in HepG2 Cells. cDNAs encoding full-length human SLC7A11 were obtained from Open Biosystems (Huntsville, AL) and subcloned into the pBabe-Puro expression vector (Addgene, Cambridge, MA) and packaged into retrovirus by transient transfection of 293T cells as described previously (Venkateswaran et al., 2000). HepG2 cells were infected at 50% confluence with the recombinant retrovirus. Stable cell lines were selected with puromycin (2 μg/ml).

Real-Time Quantitative Reverse Transcription-PCR. The effects of siRNA down-regulation and ectopic expression were detected by real-time RT-PCR and described previously (Huang et al., 2005a). The primers for SLC7A11 were 5′-TGCTGGGCTGATTTATCTTCG-3′ (forward) and 5′-GAAAGGGCAACCATGAAGAGG-3′ (reverse). The primers for β-actin were 5′-CCTGGCACCCAGCACAAT-3′ and 5′-GCCGATCCACACGGAGTACT-3′. Relative gene expression was measured with the ABI 7000 Sequence Detection system (Applied Biosystems). All amplification controls and samples were performed in triplicate and repeated at least twice.

Western Blot. Cells were lysed in lysis buffer (20 mM Tris, pH 8.0, 150 mM NaCl, 10% glycerol, 1% NP40, and 0.42% NaF) containing 1 mM phenylmethylsulfonyl fluoride, 1 mM Na_3VO_4, 2 μg/ml aprotinin, and 5 μg/ml leupeptin. Proteins were separated by gel electrophoresis on 7.5% polyacrylamide gels transferred to nitrocellulose membranes (Whatman Schleicher and Schuell, Dassel, Germany), and detected by immunoblotting using an enhanced chemiluminescence system (Alpha Innotech, San Leandro, CA). SLC7A11 antibody (1:400 dilution) was purchased from Novus (Littleton, CO). The data were analyzed by scanning densitometry and quantified using Chemiimager 4400 software (Alpha Innotech). SLC7A11 expression levels were quantified in comparison with the β-actin bands.

ROS Determination. Dichlorodihydrofluorescein diacetate (H_2DCFDA) (Molecular Probes, Eugene, OR), a nonpolar compound, can be converted into its nonfluorescent polar derivative dichlorodihydrofluorescein by cellular esterases after incorporation. Dichlorodihydrofluorescein is membrane-impermeable and rapidly oxidized to the highly fluorescent 2′,7′-dichlorofluorescein in the presence of intracellular ROS (Lai et al., 2003). Cells were treated with 1.25 μM GA or 17-AAG for 16 h followed by incubation with 5 μM H_2DCFDA in medium for 20 min at 37°C in the dark. The cells were trypsinized, washed, and resuspended in PBS. Cellular fluorescence was measured using flow cytometry performed on a fluorescence-activated cell sorter (FACScan; BD Biosciences, San Jose, CA) (excitation at 488 nm and emission at wavelengths 530 ± 15 nm) and analyzed by using CellQuest software. To study the effects of NAC on ROS production induced by GA and 17-AAG, cells were treated in combination with NAC (1 mM) and GA analogs. To determine intracellular superoxide production, we used dihydroethidium (Molecular Probes), a cell-permeant dye that is oxidized by superoxide to yield fluorescent ethidium bromide, which intercalates with nuclear DNA (Dikalov et al., 2002). Cells were rinsed with PBS and incubated with 10 μM dihydroethidium in PBS for 30 min at 37°C in the dark before FACS analysis.

Results

Clustering of 18 GA Analogs Based on Structure and Activity. Searching through ~43,000 compounds in the September 2003 release of the NCI antitumor drug screening database, we identified 18 GA analogs according to a common chemical substructure, the benzoquinone ansamycin moiety (Table 1). We performed cluster analysis for the 18 GA analogs based on similarities or differences in chemical structures (see *Materials and Methods*). They were grouped into two clusters that were characterized by C-17 substituents (Table 1). The first cluster has 10 compounds containing a methoxy group or unsubstituted at C-17, named as the "17-O/H" cluster (e.g., GA, NSC 658514, and 661581); the second cluster has 8 compounds containing various amino groups at C-17, the "17-N" cluster (e.g., 17-AAG and 17-DMAG).

Patterns of growth inhibitory activity of compounds against the NCI-60 panel have been shown to be associated with mechanisms of action (MOAs), modes of resistance, and molecular structures (Keskin et al., 2000). We therefore used PCA to classify the 18 GA analogs based on their GI_{50} values on the NCI-60. This also resulted in a separation of the GA analogs by their C-17 substituents, with 17-O/H clearly separated from 17-N analogs (Fig. 1). Although all GA analogs similarly inhibit Hsp90, the different activity patterns for the subgroups 17-O/H and 17-N may result from the differential interactions of compounds with one or more molecular targets. This suggests that 17-O/H and 17-N analogs may have different MOAs and modes of resistance.

Five compounds were available for experimental investi-

gation, including three 17-O/H analogs [i.e., the parent compound GA (NSC 122750), NSC 658514, and 661581] and the two 17-N analogs [17-AAG (NSC 330507) and 17-DMAG (NSC 707545)]. 17-AAG carries an alkylamino group in place of the methoxy moiety at C-17 (R1) of GA (Table 1). Compound 17-DMAG also differs from GA in the side chain at C-17, carrying a diamine with a two-carbon spacer between the nitrogen atoms. NSC 658514 and NSC 661581 differ from GA in the side chain of R6, but retain the methoxy moiety at C-17. Also included in our experimental investigations are two novel derivatives of 17-AAG, 17-AEP-GA and 17-DMAP-GA (not shown in Table 1); growth inhibitory activity data for these two compounds are not available in the NCI-60 database. 17-AEP-GA and 17-DMAP-GA, similar to 17-AAG and 17-DMAG, have been synthesized by replacing the C-17 methoxy moiety with alkylamino groups; they therefore belong to the 17-N group (Tian et al., 2004).

Correlation of SLC7A11 Gene Expression with Growth Inhibitory Potency of GA Analogs. The mRNA expression was previously measured in the NCI-60 cell panel with a customized microarray containing oligonucleotide probes targeting the majority of transporter genes presently known to be relevant to drug transport (Huang et al., 2004). To identify genes potentially involved in sensitivity and resistance to GA analogs, we first performed correlation analysis between the microarray gene expression profiles and growth inhibitory activity of six GA analogs across the NCI-60. SLC7A11 and SLC3A2 were two of the five transporter genes showing significant GA correlations identified from the systematic screening (Huang et al., 2007). We next performed correlation analysis between gene expression of SLC7A11 and growth inhibitory potency of 18 GAs across the NCI-60. This yielded Pearson correlation coefficients (r) for each gene-drug pair. The statistical significance of the correlation for each gene-drug pair was assessed by computing unadjusted bootstrap p values (Efron and Tibshirani, 1993).

All 18 analogs showed negative SLC7A11 correlations (Fig. 2A). Significant negative correlations indicative of chemoresistance occur between SLC7A11 gene expression and 8 of 10 17-O/H compounds. However, only one of eight 17-N analogs showed significant negative correlations with SLC7A11. The drug correlation profiles were similar for SLC3A2, which showed significant negative correlations with 6 of 10 17-O/H analogs, but not with 17-N analogs (data not shown). Figure 2B shows a representative relationship between SLC7A11 level and growth inhibitory potency for GA and 17-AAG. Several cell lines (A549, HOP-62, H322M, and SK-OV-3) that have relatively high expression of SLC7A11 and are resistant to GA are highlighted. In contrast, these cell lines are not resistant to 17-AAG. The mean SLC7A11 correlation was −0.40 for the 17-O/H cluster, and −0.10 for the 17-N cluster. A Student's t test supported the alternative hypothesis, $\text{mean}_{17\text{-O/H}} < \text{mean}_{17\text{-N}}$ with p value of 0.0012. If there were a connection between drug resistance and SLC7A11 expression level, we would expect to detect a difference in compound potency between cell lines over- and underexpressing this

TABLE 1

Chemical structures of GA and its analogs

Cluster analysis based on similarities or differences in chemical structures grouped these analogs into two subgroups which were characterized by the C-17 substituents (R_1): 17-O/H (in bold, 10 compounds), 17-N (eight compounds). 17-O/H analogs contain a methoxy or hydroxy group or unsubstituted at C-17, whereas the 17-N group contains various amino groups at the C-17. Five analogs in italic are those available for experimental validation.

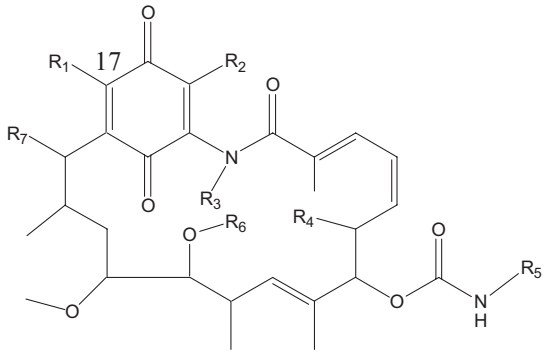

NSC	Name	R_1	R_2	R_3	R_4	R_5	R_6	R_7
122750	GA	OMe	H	H	OMe	H	H	H
658514		OMe	H	H	OMe	H	$C(=O)(CH_2)_3NH_2$	H
661581		OMe	H	H	OMe	H	$C(=O)(CH_2)_2NH_2$	H
210753		OMe	CH = N-t-Bu	H	OMe	H	H	H
255111		OMe	CH = N-C_5H_{10}N	H	OMe	H	H	H
330512		OMe	H	Me	OMe	Me	H	H
661580		OMe	H	H	OMe	H	$C=(O)CH_2NH_2$	H
255104		OH	H	H	OMe	H	H	H
305978	Herbimycin	H	H	H	Me	H	Me	OMe
330499	Macbecin I	H	H	H	OMe	H	Me	OMe
330507	17-AAG	$NCH_2CH = CH_2$	H	H	OMe	H	H	H
707545	17-DMAG	$NCH_2CH_2NMe_2$	H	H	OMe	H	H	H
255109	17-AG	NH2	H	H	OMe	H	H	H
320877		NCH_2CH_2Cl	H	H	OMe	H	H	H
683661		$NCH_2CH = CH_2$	H	H	OMe	H	$C=(O)CH_2NH_2$	H
683662		$NCH_2CH = CH_2$	H	H	OMe	H	$C=(O)CH_2NMe_2$	H
683663		$NCH_2CH = CH_2$	H	H	OMe	H	$C(=O)(CH_2)_2NH_2$	H
683664		$NCH_2CH = CH_2$	H	H	OMe	H	$C(=O)(CH_2)_2NMe_2$	H

gene. To corroborate GA-SLC7A11 correlations, we calculated the difference in cytotoxic potency between two lung cancer cell lines HOP-62 and HOP-92. HOP-62 expresses relatively high levels of SLC7A11, whereas HOP-92 does not (Huang et al., 2005a). For both compound clusters, we calculated the mean difference in potency between the two cell lines. On average, the 17-O/H analogs are approximately 6.6 times less potent against HOP-62 than HOP-92, whereas the 17-N analogs are approximately 7.2 times more potent against HOP-62 than HOP-92. A Student's t test supported the alternative hypothesis ($p < 0.0001$). Therefore, the structural and potency classification (shown in Fig. 1 and Table 1) may relate to SLC7A11 correlations (shown in Fig. 2) and associate with the pharmacological features of these compounds due to the importance of the C-17 position. Because small differences in chemical structure may determine whether a compound is subject to SLC7A11 and GSH mediated resistance (Dai et al., 2007), we subsequently studied representative compounds in the two clusters regarding to the interactions with SLC7A11.

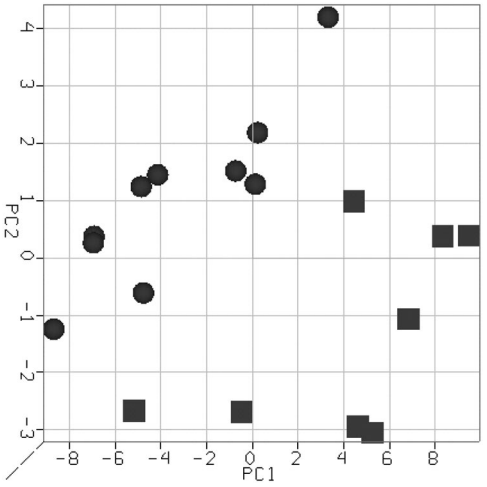

Fig. 1. PCA of 18 GA analogs based on their growth inhibitory potency (GI_{50} values) across the NCI-60. The location was based on the first three principal components using the GI_{50} values for the 18 GA analogs. Compounds are labeled according to the classification obtained based on chemical structures. Each sphere represents a 17-O/H analog. Each cube represents a 17-N analog.

Evidence that SLC7A11 Confers Resistance to 17-O/H but Not to 17-N Analogs. To validate various correlations between SLC7A11 and GA analogs, we used lung cancer A549 cells, which express relatively high levels of SLC7A11 and are relatively more resistant to GA (Fig. 2B), and compared the drug sensitivity with and without inhibition of SLC7A11 activity. The cells were first exposed to 4-*S*-CPG, a specific inhibitor of system x_c^- (Patel et al., 2004) to inhibit cystine influx and lower the intracellular GSH levels (Huang et al., 2005a). As shown in Fig. 3A and Table 2, the presence of 50 uM 4-*S*-CPG sensitized the cells to GA, NSC 658514, and NSC 661581, representatives for the 17-O/H analogs. 4-*S*-CPG had no affect on the potencies of 17-N analogs, such as 17-AAG, 17-DMAG, 17-AEP-GA, and 17-DMAP-GA. Cells were also exposed to 5 mM glutamate to

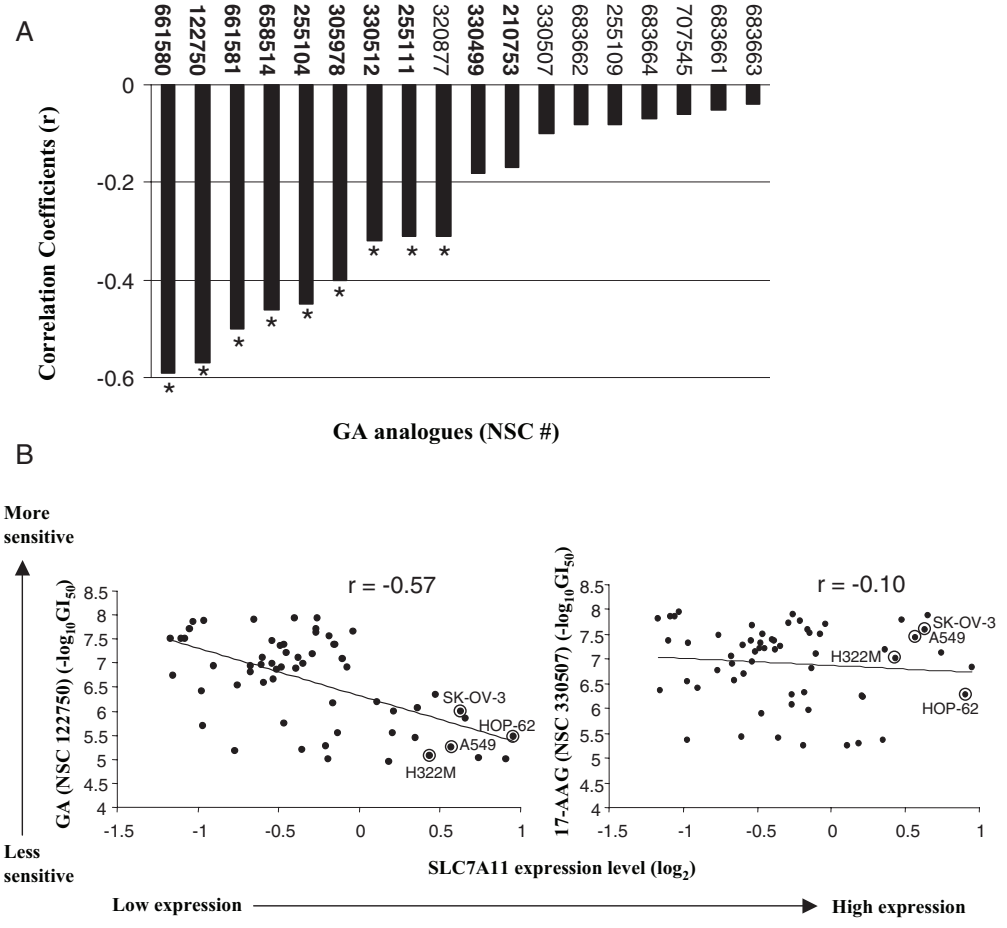

Fig. 2. Correlation between SLC7A11 expression and growth inhibitory potency of 18 GA analogs in the NCI-60. A, plot of sorted Pearson correlation coefficients (r) between gene expression of SLC7A11 and cytotoxic potencies of 18 GA analogs. *, $P < 0.05$. 17-O/H compounds are in bold. B, scatter plots showing the correlation (r) of SLC7A11 expression with chemosensitivity of the NCI-60 cell lines to GA and 17-AAG. A $\log_{10}GI_{50}$ value of 1 for sensitivity indicates a 10-fold difference in the sensitivity to the drug. The SLC7A11 level is plotted as the abundance ($\log_2$) of the SLC7A11 mRNA transcript, relative to its abundance in the reference pool of 12 cell lines. The circles indicate four cell lines selected for the experiments that have relatively high expression of SLC7A11 and are relatively more resistant to GA.

inhibit SLC7A11 activity (Huang et al., 2005a), yielding the same results as 4-*S*-CPG (data not shown). We next compared drug potencies of SLC7A11 siRNA-treated cells with those of nonsilencing control siRNA-treated cells. SLC7A11 siRNA resulted in >80% reduction in SLC7A11 mRNA levels revealed by real-time RT-PCR analysis (Supplementary Fig. 1). For siRNA down-regulation we obtained results similar to those for SLC7A11 inhibitors (Fig. 3B and Table 2).

The hepatocarcinoma cell line HepG2 showed a higher sensitivity to GA (IC_{50}, 4.2 ± 0.027 nM) compared with A549 (IC_{50}, 24 ± 0.022 nM). The expression of SLC7A11 in A549 was 4 and 1.7 times that in HepG2 cells at mRNA and protein levels, respectively (Fig. 4, A and C). To confirm the role of SLC7A11 in cellular resistance to cytotoxicity, HepG2 cells were infected with the retrovirus containing pBabe expression vector to create a cell line stably expressing either vector alone or SLC7A11 cDNA. Real-time quantitative RT-PCR showed that the HepG2/SLC7A11 cells expressed 12-fold more SLC7A11 mRNA than HepG2 cells infected with the vector (Fig. 4B). Western blot analysis showed a 6.5-fold increase of SLC7A11 protein in the HepG2/SLC7A11 cells (Fig. 4C). The cytotoxicity of GA and 17-AAG in HepG2/SLC7A11 cells was compared with that of vector-infected HepG2 cells. The sensitivity of HepG2/SLC7A11 cells to GA was significantly reduced [IC_{50}(HepG2/SLC7A11)/IC_{50}(HepG2/vector) = 3.2, $P < 0.05$] (Fig. 5A). However, for 17-AAG, the cytotoxicity to HepG2/

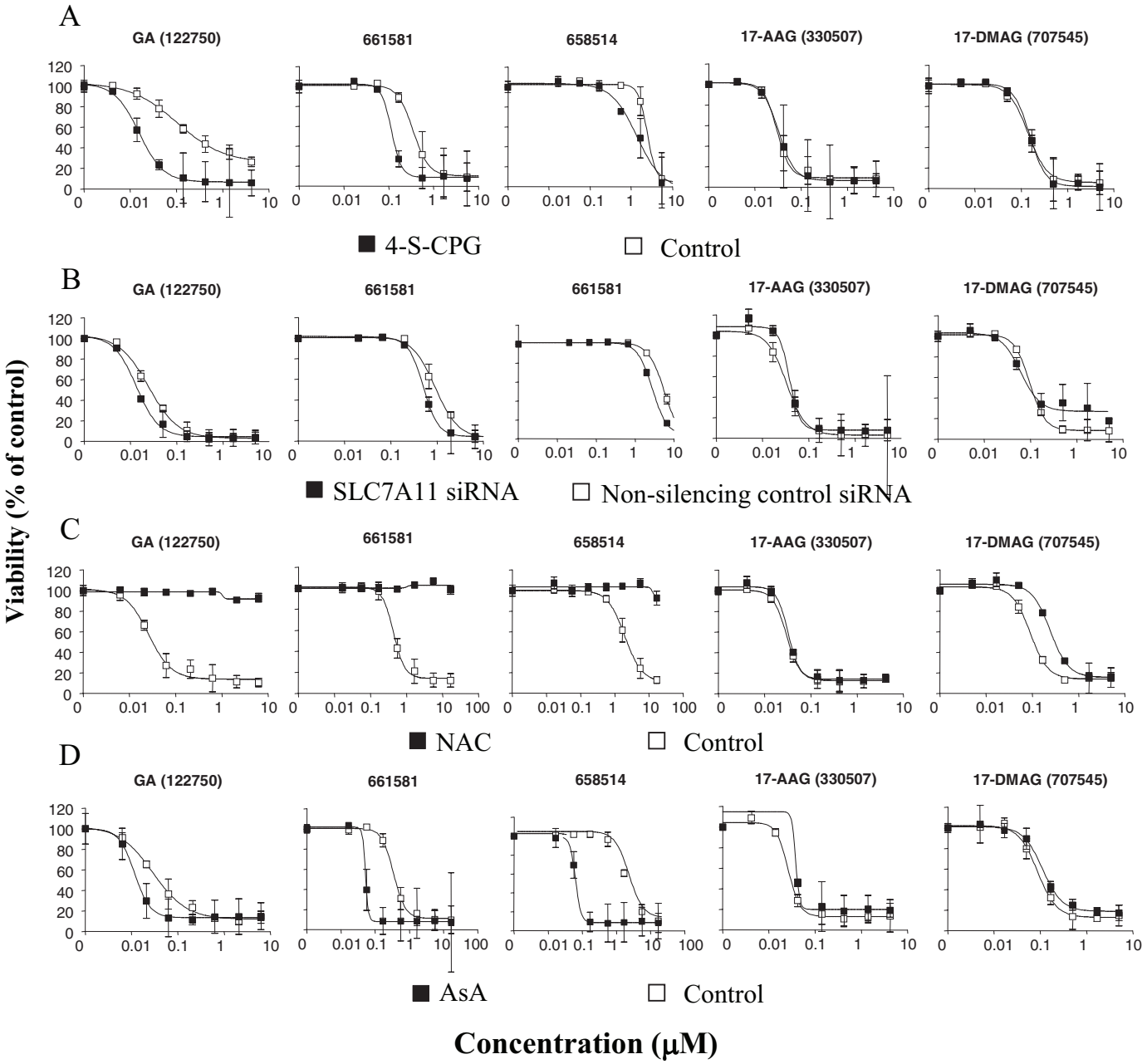

Fig. 3. Functional validation of the SLC7A11-GA correlations. A, growth inhibition curves for A549 cells in response to GA, NSC 661581 and 658514, 17-AAG and 17-DMAG with or without treatment with the system x_c^- inhibitor 4-*S*-CPG (50 μM). B, effect of down-regulation of SLC7A11 by siRNA or nonsilencing control siRNA on drug sensitivity of A549 cells. C, chemosensitivity of A549 cells with or without treatment with the GSH precursor, an antioxidant NAC (1 mM). D, chemosensitivity of A549 cells with or without treatment with the prooxidant AsA (1 mM). Results are expressed as percentage survival of control cells with no drug treatment (means ± S.D. from three replicates).

SLC7A11 cells and the parent cells did not show significant difference [IC_{50}(HepG2/SLC7A11)/IC_{50}(HepG2/vector) = 1.6, $P = 0.36$] (Fig. 5B). These data support the idea that SLC7A11 plays a different role in the resistance to GA and 17-AAG.

The role of SLC7A11 in chemoresistance seems to be mediated by GSH. In a previous study, we have treated the A549 and SK-OV-3 cells with buthionine sulfoximine, the specific inhibitor of the rate-limiting enzyme in the synthesis of GSH, γ-glutamylcysteine synthetase (γ-GCS), to compare the effects of suppressing SLC7A11 transport activity with those of inhibiting GSH synthesis via a different path. Buthionine sulfoximine treatment strongly sensitized the A549 cells to GA, but the effects on 17-AAG were much smaller (Huang et al., 2005a). Here, we further performed a study evaluating the effects of NAC, a precursor of cysteine and GSH synthesis, in modulating the chemosensitivity to GA analogs. As shown in Fig. 3C and Table 2, the presence of NAC (1 mM) completely blocked the cytotoxic effects of GA, NSC 658514, and 661581, but with no or much smaller protective effect on 17-AAG and other 17-N compounds. To determine whether the effects of NAC were broadly observed, we performed a similar study on HepG2 cells as well and obtained results similar to those in A549 cells (data not shown).

The functions of GSH and NAC involve a variety of mechanisms, among which is scavenging ROS. We therefore tested the effects of ascorbic acid (AsA, or vitamin C), a pro-oxidant rather than an antioxidant (D'Agostini et al., 2005), on the

TABLE 2

Effects of 4-S-CPG, SLC7A11-specific siRNA, NAC, and AsA on cytotoxicity of GA analogs in A549 cells

4-S-CPG (50 μM) was used to suppress SLC7A11 transport activity. siRNA was used to downregulate SLC7A11 expression. The effects of the GSH precursor and antioxidant NAC (1 mM) and the prooxidant AsA (1 mM) were also tested on the cytotoxicity of GA analogs. IC_{50} values in micromolar are shown for each drug in the presence or absence of 4-S-CPG, siRNA, NAC, or AsA. Values in the rows marked "-Fold" are -fold reversal, which is the IC_{50} for the cytotoxic drug in control cells divided by that in inhibitor-treated cells. When IC_{50} was higher than the maximum concentration used, it is denoted as "> maximum concentration," and the -fold changes were calculated using the maximum concentration. Results represent mean ± S.D. of at least three experiments.

NSC #	122750	658514	661581	330507	707545		
Name	GA			17-AAG	17-DMAG	17-AEP-GA	17-DMAP-GA
CC	−0.57	−0.46	−0.50	−0.10	0.06		
−4-S-CPG	0.026 ± 0.00	2.5 ± 0.51	0.35 ± 0.05	0.086 ± 0.01	0.15 ± 0.00	0.072 ± 0.01	0.31 ± 0.02
+4-S-CPG	0.004 ± 0.00	1.6 ± 0.40	0.12 ± 0.01	0.062 ± 0.00	0.14 ± 0.02	0.082 ± 0.00	0.34 ± 0.04
-Fold	(7.1)*	(1.6)*	(3.0)*	(1.4)	(1.1)	(0.89)	(0.94)
−siRNA	0.025 ± 0.00	5.9 ± 0.33	0.92 ± 0.13	0.03 ± 0.00	0.10 ± 0.00	0.030 ± 0.00	0.11 ± 0.01
+siRNA	0.013 ± 0.00	2.8 ± 0.11	0.51 ± 0.03	0.04 ± 0.00	0.10 ± 0.01	0.017 ± 0.00	0.083 ± 0.03
-Fold	(1.8)*	(2.1)*	(1.8)*	(0.9)	(1.0)	(1.8)	(1.4)
−NAC	0.026 ± 0.00	2.0 ± 0.35	0.45 ± 0.05	0.033 ± 0.00	0.090 ± 0.01	0.057 ± 0.01	0.14 ± 0.01
+NAC	>6.25	>16.7	>16.7	0.030 ± 0.00	0.24 ± 0.01	0.15 ± 0.05	0.26 ± 0.02
-Fold	(<0.0042)*	(<0.12)*	(<0.027)*	(1.1)	(0.37)*	(0.42)	(0.54)*
−AsA	0.029 ± 0.00	1.9 ± 0.18	0.35 ± 0.03	0.026 ± 0.00	0.088 ± 0.01	0.047 ± 0.01	0.11 ± 0.00
+AsA	0.012 ± 0.00	0.063 ± 0.00	0.051 ± 0.00	0.038 ± 0.00	0.11 ± 0.01	0.057 ± 0.01	0.28 ± 0.04
-Fold	(2.5)*	(30)*	(6.8)*	(0.69)*	(0.78)	(0.82)	(0.41)*

CC, Pearson correlation coefficients between compound potency and SLC7A11 expression.
* $P < 0.05$ versus controls without adding inhibitors or siRNA.

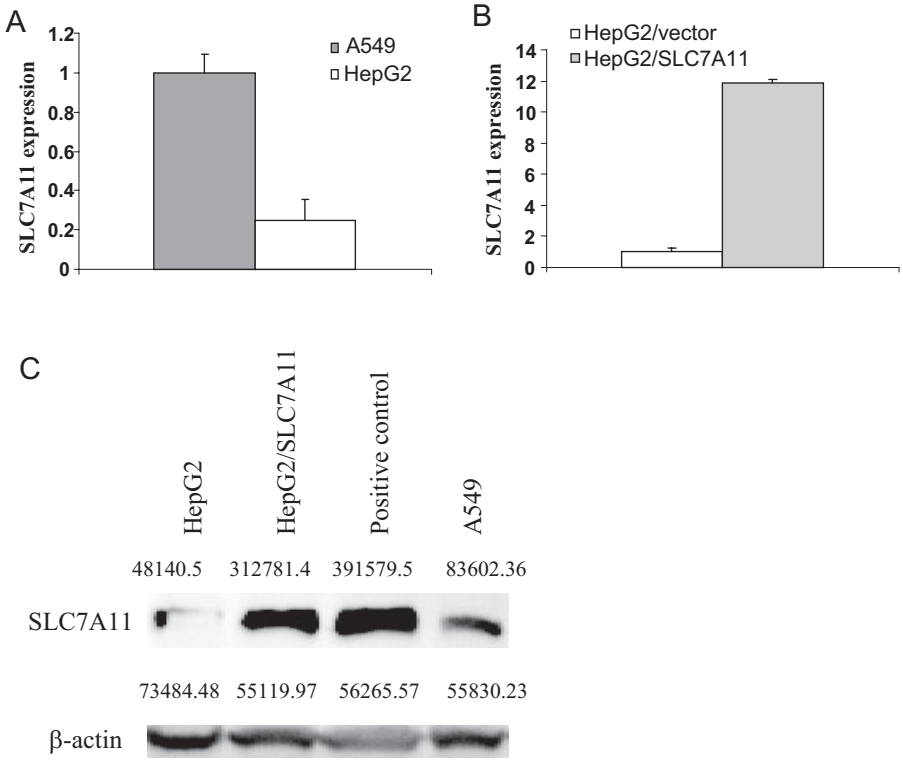

Fig. 4. Expression analysis of SLC7A11 detected by quantitative real-time RT-PCR and Western blot. A, real-time RT-PCR analysis to compare the basal SLC7A11 levels in A549 and HepG2 cells. Relative gene expression is shown (SLC7A11 level in A549 cells was set at 1). Expression levels were normalized to the β-actin levels. Each reaction was performed in triplicate. The SLC7A11 mRNA in HepG2 cells was 25% of that in A549 cells. B, real-time RT-PCR results of SLC7A11 levels in HepG2 infected with pBabe retroviral vector containing SLC7A11 cDNA (HepG2/SLC7A11) and HepG2 infected with empty vector (HepG2/vector). HepG2/SLC7A11 expressed nearly 12-fold more SLC7A11 mRNA than the parent cells. Expression levels of β-actin were used for normalization. C, expression of SLC7A11 protein was detected by Western blot analysis (a single 55-kDa band). Compared with A549 cells, HepG2 expresses less SLC7A11. The level of SLC7A11 expression in HepG2/SLC7A11 cells was much higher than the parent cells. Quantification of the band intensity is shown for each band. A mesothelioma cell line was used as the positive control.

sensitivity to GA analogs. AsA has been shown to increase intracellular ROS levels and induce apoptosis of tumors, which was preventable by pretreatment with NAC (Inai et al., 2005). In contrast to the effects of NAC, administration of AsA (1 mM) considerably and significantly potentiated the cytotoxicity of GA, NSC 658514, and 661581, but for 17-N compounds, it had either no sensitizing effect or mildly reduced the sensitivity for some of them (Fig. 3D and Table 2). Thus, the antioxidant NAC and the prooxidant AsA displayed opposite modulation of chemosensitivity to GA analogs. The effects of NAC and AsA seem to correlate with classification of GA analogs based on chemical structure and potency. To determine whether the observed results were cell line-specific phenomena or broadly applicable, we similarly tested the effects of 4-*S*-CPG, glutamate, NAC, and AsA on lung cancer HOP-62 and H322M cells and ovarian cell line SK-OV-3, which express relatively high levels of SLC7A11 (Fig. 2B). The results were consistent in all cell lines tested (data not shown).

Effects of GA and 17-AAG on ROS Production in A549 and HepG2 Cells. SLC7A11/GSH-mediated chemoresistance and protection of cytotoxicity by the antioxidant NAC suggest a role for ROS in induction of cytotoxicity by the 17-O/H analogs. This hypothesis led us to identify and quantitate intracellular ROS levels after administration of GA or 17-AAG. The cell-permeable fluorescent dye H_2DCFDA was used to measure intracellular ROS levels. The dye can be oxidized by intracellular ROS to generate a fluorescent product measurable to give an estimation of intracellular ROS status. ROS production was low in untreated cells at basal level. However, it became significantly elevated at 16 h after GA treatment of A549 and HepG2 cells ($P < 0.05$) (Fig. 6). Induction of ROS by GA was significantly higher than that by 17-AAG in both cell lines ($P < 0.05$). 17-AAG did not increase ROS levels in A549 cells, but in HepG2 cells, ROS was elevated. ROS induction by GA was completely suppressed by NAC, which therefore confirmed the blocking effect of NAC on cytotoxicity of GA. The effects of GA and 17-AAG on superoxide production were also studied with an established method involving oxidation of dihydroethidium. Treatment of A549 and HepG2 cells with GA significantly increased the amount of superoxide detected by dihydroethidium compared with 17-AAG treatment and the untreated controls (data not shown). Thus, the tumor cytotoxic effects of the 17-O/H analogs, but not the 17-N analogs, might be ROS-dependent. This may account for differential relationship of 17-O/H and 17-N analogs with SLC7A11 and indicate that 17-N analogs can bypass the resistance mechanism.

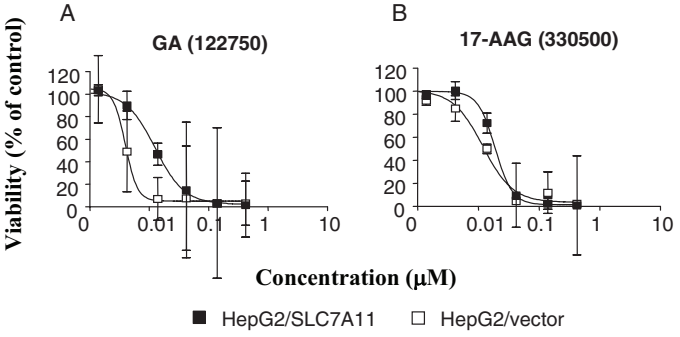

Fig. 5. Cytotoxicity of GA (A) and 17-AAG (B) in HepG2 with ectopic SLC7A11 expression and the control HepG2 cells. Cytotoxicity of GA and 17-AAG were measured by SRB assay in HepG2 cells infected with a retrovirus containing pBabe vector alone or SLC7A11 cDNA and selected with 2 μg/ml puromycin. Results are expressed as percentage survival of control cells with no drug treatment (means ± S.D. from three replicates).

Discussion

This study emerged from a pharmacogenomic investigation, in which we analyzed the correlations between mRNA expression profiles of human transporter genes and patterns of growth inhibitory potency of the anticancer drug GA in the NCI-60 panel (Huang et al., 2004, 2007). The power of this pharmacogenomic approach has been demonstrated by identification of several transporter genes conveying varying degrees of chemoresistance to different anticancer drugs with the aid of in vitro manipulation of transporter activities using transporter-specific inhibitors or siRNA (Huang et al., 2005a,b; Dai et al., 2007). The present study followed up on our previous work (Huang et al., 2007) and focused on the amino acid transport system x_c^-, a heterodimer encoded by two genes in the solute carrier superfamily, SLC7A11 and SLC3A2, for the light (or catalytic chain) and heavy chain of system x_c^-, respectively. System x_c^- plays an important role in maintaining cellular GSH levels and mediating chemoresistance to cytotoxic agents (Huang et al., 2005a).

We examined the potential links between the amino acid transport system x_c^- (represented by SLC7A11) and cytotoxicity to a panel of GA analogs. In one of our previous studies, GA was identified as the candidate anticancer drug with negative SLC7A11 correlation (Huang et al., 2005a). Although closely related in structural properties, GA analogs differ widely in their correlations with SLC7A11 expression. The present study shows that SLC7A11 conveys resistance to

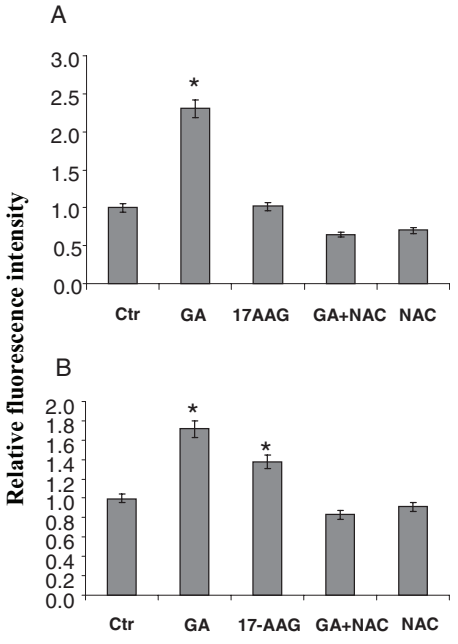

Fig. 6. Effects of GA and 17-AAG on the production of ROS in drug-treated A549 cells (A) and HepG2 cells (B). Cells were treated with 1.25 μM GA and 17-AAG, respectively, for 16 h. ROS production in the treated cells was represented by intracellular fluorescent intensity determined by flow cytometry. The data are the means ± S.D. Similar results were obtained in three independent experiments. *, $p < 0.05$ (relative to control samples without drug treatment).

GA, NSC 658514, and NSC 661581 but not to 17-AAG, 17-DMAG, 17-AEP-GA, and 17-DMAP-GA. The 18 GA analogs can be clustered into two distinct subgroups, 17-O/H and 17-N, according to their chemical structures and potency on the NCI-60. Most of the 17-O/H analogs showed significant correlations with SLC7A11 expression, whereas no significant SLC7A11 correlation was observed with most of the 17-N analogs. This suggested that the two subgroups have distinct MOAs and modes of resistance. This notion was supported by a variety of methods—by pharmacologic inhibition of SLC7A11, siRNA-mediated down-regulation of SLC7A11, overexpression of SLC7A11, and toxicity profiles of cell lines with high versus low endogenous SLC7A11 expression. The basis for this difference could be that SLC7A11 plays an important role in maintenance of cellular GSH levels and that 17-O/H drugs induce higher levels of ROS compared with 17-N derivatives. This notion was further supported by addition of either NAC, an antioxidant, or AsA, a prooxidant, in combination with GA analogs. NAC dramatically increased the IC_{50} of GA but had minimal effects upon 17-AAG and other 17-N analogs. AsA reduced the IC_{50} of GA but did not reduce the values for 17-AAG and related agents. 17-AEP-GA and 17-DMAP-GA are new GA analogs with the alkylamino group in place of the methoxy moiety at C-17. They were shown to induce tumor cell growth inhibition similar to that induced by 17-AAG but with better water solubility (Tian et al., 2004). According to their structural features, they can be grouped as the "17-N" analogs. Our data showed that they have an SLC7A11 relationship similar to that of 17-AAG and 17-DMAG. Thus, we used 17-AAG or 17-DMAG as representatives for the 17-N group because they are currently in clinical trials. These results have important implications, because SLC7A11 may serve as a biomarker for predicting efficacy of a panel of anticancer drugs and selecting optimal drug therapies for individual tumors. For this purpose, the role of SLC7A11 needs to be tested against more analogs of GA or other compound classes in more cell types.

The transport system x_c^- is a heterodimeric complex composed of SLC7A11 and SLC3A2. It is clear that SLC3A2 is required for proper cell surface localization of SLC7A11 and for its transport function. One would expect that in HepG2, the optimal expression and proper function of SLC7A11 will require SLC3A2. We manipulated HepG2 cells only with SLC7A11 overexpression, because it was reported that in NIH3T3 cells transfected with SLC7A11 cDNA alone, the activity of cystine transport was significantly increased (Wang et al., 2003). However, this may account for the observation that although the increase of SLC7A11 in HepG2/SLC7A11 was high (12-fold), the change of potency for GA was only 3.2-fold (Fig. 5). It may be important to know whether the levels of endogenous SLC3A2 are sufficient for proper localization and functioning of SLC7A11 in HepG2 cells and other cells with low levels of SLC7A11.

There are two possibilities for the connection between SLC7A11/GSH and chemoresistance. First, GSH forms drug conjugates, which commonly renders the compounds less cytotoxic, facilitates transport out of the cells, or prevents binding to the target (Hsp90). Two recent reports showed that GA, 17-AAG, and 17-DMAG could react chemically (i.e., nonenzymatically) with GSH (Cysyk et al., 2006; Lang et al., 2007). Although the conjugation proceeds rapidly with GA and less rapidly with 17-DMAG and 17-AAG, the latter can also form GSH conjugates. In addition, we found that MRP1 encoded by the *ABCC1* gene, an efflux transporter for GSH conjugated compounds, mediates efflux and resistance to both 17-O/H and 17-N compounds (A.-N. Pham and Y. Huang, unpublished results). Therefore, GSH conjugation may not fully explain the difference. Second, GSH plays a prominent role in a cellular defense against ROS. In fact, system x_c^- can be adaptively induced in response to oxidative stress and thereby closely associated with the cellular antioxidant machinery (Sasaki et al., 2002). SLC7A11 has been shown to play a pivotal role in maintaining redox balance and protection from oxidative stress based on the results from SLC7A11−/− mice (Sato et al., 2005). In the present study, GA and 17-AAG showed difference in generation of ROS: GA produced significantly higher levels of intracellular superoxides and H_2O_2. It has consistently been shown that treatment of endothelial cells with GA resulted in a dramatic increase in superoxide formation by redox cycling, an effect independent of Hsp90 inhibition (Dikalov et al., 2002), whereas, to our knowledge, there has been no report of 17-N analogs producing ROS. Therefore, our data not only support a SLC7A11-mediated resistance mechanism that is specifically directed toward 17-O/H analogs but also suggest a differential role of ROS in the cytotoxic activity between the two subgroups of compound. The strong correlations between SLC7A11 and 17-O/H analogs in NCI-60 panel could have resulted from the fact that cancer cells expressing high levels of SLC7A11 have a high antioxidant potential, producing or maintaining more GSH, which scavenges ROS and/or forms GSH conjugates, and therefore are more resistant to cytotoxic effects of 17-O/H analogs. In contrast, cell lines with low level of SLC7A11 cannot produce sufficient GSH and might be more sensitive to ROS-producing compounds. The cytotoxic effects of 17-O/H analogs may depend on ROS production, whereas ROS may not be important for 17-N analogs, which therefore bypass the resistance mechanism mediated by SLC7A11. However, to distinguish between the possibilities of GSH conjugation and ROS scavenging, further experiments should be done to examine the ability of 17-O/H analogs to target Hsp90 in the presence of GSH and perform drug transport study in the presence or absence of GSH.

Several genes and proteins have been previously associated with sensitivity to GA analogs, including expression levels or mutation status of key Hsp90 client proteins such as ERBB2, BRAF, Bcr-Abl, and AKT (da Rocha Dias et al., 2005; Demidenko et al., 2005) as well as levels of Hsp90 family members such as Hsp70 (Guo et al., 2005). For 17-AAG, the metabolizing enzyme NAD(P)H:quinone oxidoreductase 1 was found important for tumor cell sensitivity (Kelland et al., 1999). Moreover, elevated expression of the ATP-binding cassette transporter gene *ABCB1* (MDR1 or P-glycoprotein) contributes to tumor resistance to some of the GA analogs (Huang et al., 2004, 2007). Thus, like other commonly used anticancer agents, multiple factors contribute to the cellular sensitivity and resistance to GA analogs. There is a surprising coherence between SLC7A11-correlations and the degree of hepatotoxicity of these compounds: 17-O/H analogs, such as GA, showed strong hepatotoxicity and are more hepatotoxic than 17-N analogs in preclinical studies (Uehara, 2003). Thus, system x_c^- and GSH could play a role in modulating hepatotoxicity and could therefore be factors determining the

differential toxicity of the analogs observed in preclinical studies.

Acknowledgments

We thank the staff of NCI DTP for generation of the pharmacological database used in this study. We thank Dr. Leming Shi (NCTR/FDA) for providing comments on the manuscript and Feng Qian and Hong Fang (NCTR/FDA) for assistance in ArrayTrack analysis.

References

Blower PE Jr, Cross KP, Fligner MA, Myatt GJ, Verducci JS, and Yang C (2004) Systematic analysis of large screening sets. *Curr Drug Discov Technol* **1:**37–47.

Blower PE, Yang C, Fligner MA, Verducci JS, Yu L, Richman S, and Weinstein JN (2002) Pharmacogenomic analysis: correlating molecular substructure classes with microarray gene expression data. *Pharmacogenomics J* **2:**259–271.

Cysyk RL, Parker RJ, Barchi Jr JJ, Steeg PS, Hartman NR, and Strong JM (2006) Reaction of geldanamycin and C17-substituted analogues with glutathione: product identifications and pharmacological implications. *Chem Res Toxicol* **19:**376–381.

da Rocha Dias S, Friedlos F, Light Y, Springer C, Workman P, and Marais R (2005) Activated B-RAF is an Hsp90 client protein that is targeted by the anticancer drug 17-allylamino-17-demethoxygeldanamycin. *Cancer Res* **65:**10686–10691.

D'Agostini F, Balansky RM, Camoirano A, and De Flora S (2005) Modulation of light-induced skin tumors by *N*-acetylcysteine and/or ascorbic acid in hairless mice. *Carcinogenesis* **26:**657–664.

Dai Z, Barbacioru C, Huang Y, and Sadee W (2006) Prediction of Anticancer drug potency from expression of genes involved in growth factor signaling. *Pharm Res* **23:**336–349.

Dai Z, Huang Y, Sadee W, and Blower P (2007) Chemoinformatics analysis identifies cytotoxic compounds susceptible to chemoresistance mediated by glutathione and cystine/glutamate transport system xc. *J Med Chem* **50:**1896–1906.

Demidenko ZN, An WG, Lee JT, Romanova LY, McCubrey JA, and Blagosklonny MV (2005) Kinase-addiction and biphasic sensitivity-resistance of Bcr-Abl- and Raf-1-expressing cells to imatinib and geldanamycin. *Cancer Biol Ther* **4:**484–490.

Dikalov S, Landmesser U, and Harrison DG (2002) Geldanamycin leads to superoxide formation by enzymatic and non-enzymatic redox cycling. Implications for studies of Hsp90 and endothelial cell nitric-oxide synthase. *J Biol Chem* **277:**25480–25485.

Efron B and Tibshirani R (1993) *An Introduction to the Bootstrap.* Chapman Hall, New York.

Everitt BS (1993) *Cluster Analysis.* Halsted Press, New York.

Gatti L and Zunino F (2005) Overview of tumor cell chemoresistance mechanisms. *Methods Mol Med* **111:**127–148.

Guo F, Rocha K, Bali P, Pranpat M, Fiskus W, Boyapalle S, Kumaraswamy S, Balasis M, Greedy B, Armitage ES, et al. (2005) Abrogation of heat shock protein 70 induction as a strategy to increase antileukemia activity of heat shock protein 90 inhibitor 17-allylamino-demethoxy geldanamycin. *Cancer Res* **65:**10536–10544.

Huang Y and Sadee W (2003) Drug sensitivity and resistance genes in cancer chemotherapy: a chemogenomics approach. *Drug Discov Today* **8:**356–363.

Huang Y, Dai Z, Barbacioru C, and Sadee W (2005a) Cystine-glutamate transporter SLC7A11 in cancer chemosensitivity and chemoresistance. *Cancer Res* **65:**7446–7454.

Huang Y, Blower PE, Liu R, Dai Z, Pham AN, Moon H, Fang J, and Sadee W (2007) Chemogenomic analysis identifies geldanamycins as substrates and inhibitors of ABCB1. *Pharm Res* **24:**1702–1712.

Huang Y, Blower PE, Yang C, Barbacioru C, Dai Z, Zhang Y, Xiao JJ, Chan KK, and Sadee W (2005b) Correlating gene expression with chemical scaffolds of cytotoxic agents: ellipticines as substrates and inhibitors of MDR1. *Pharmacogenomics J* **5:**112–125.

Huang Y, Anderle P, Bussey KJ, Barbacioru C, Shankavaram U, Dai Z, Reinhold WC, Papp A, Weinstein JN, and Sadee W (2004) Membrane transporters and channels: role of the transportome in cancer chemosensitivity and chemoresistance. *Cancer Res* **64:**4294–4301.

Inai Y, Bi W, Shiraishi N, and Nishikimi M (2005) Enhanced oxidative stress by L-ascorbic acid within cells challenged by hydrogen peroxide. *J Nutr Sci Vitaminol (Tokyo)* **51:**398–405.

Kelland LR, Sharp SY, Rogers PM, Myers TG, and Workman P (1999) DT-Diaphorase expression and tumor cell sensitivity to 17-allylamino,17-demethoxygeldanamycin, an inhibitor of heat shock protein 90. *J Natl Cancer Inst* **91:**1940–1949.

Keskin O, Bahar I, Jernigan RL, Beutler JA, Shoemaker RH, Sausville EA, and Covell DG (2000) Characterization of anticancer agents by their growth inhibitory activity and relationships to mechanism of action and structure. *Anticancer Drug Des* **15:**79–98.

Lai MT, Huang KL, Chang WM, and Lai YK (2003) Geldanamycin induction of grp78 requires activation of reactive oxygen species via ER stress responsive elements in 9L rat brain tumour cells. *Cell Signal* **15:**585–595.

Lang W, Caldwell GW, Li J, Leo GC, Jones WJ, and Masucci JA (2007) Biotransformation of geldanamycin and 17-allylamino-17-demethoxygeldanamycin by human liver microsomes: reductive versus oxidative metabolism and implications. *Drug Metab Dispos* **35:**21–29.

Okuno S, Sato H, Kuriyama-Matsumura K, Tamba M, Wang H, Sohda S, Hamada H, Yoshikawa H, Kondo T, and Bannai S (2003) Role of cystine transport in intracellular glutathione level and cisplatin resistance in human ovarian cancer cell lines. *Br J Cancer* **88:**951–956.

Patel SA, Warren BA, Rhoderick JF, and Bridges RJ (2004) Differentiation of substrate and non-substrate inhibitors of transport system x_c^-: an obligate exchanger of L-glutamate and L-cystine. *Neuropharmacology* **46:**273–284.

Sasaki H, Sato H, Kuriyama-Matsumura K, Sato K, Maebara K, Wang H, Tamba M, Itoh K, Yamamoto M, and Bannai S (2002) Electrophile response element-mediated induction of the cystine/glutamate exchange transporter gene expression. *J Biol Chem* **277:**44765–44771.

Sato H, Tamba M, Kuriyama-Matsumura K, Okuno S, and Bannai S (2000) Molecular cloning and expression of human xCT, the light chain of amino acid transport system xc. *Antioxid Redox Signal* **2:**665–671.

Sato H, Shiiya A, Kimata M, Maebara K, Tamba M, Sakakura Y, Makino N, Sugiyama F, Yagami K, Moriguchi T, et al. (2005) Redox imbalance in cystine/glutamate transporter-deficient mice. *J Biol Chem* **280:**37423–37429.

Smith V, Sausville EA, Camalier RF, Fiebig HH, and Burger AM (2005) Comparison of 17-dimethylaminoethylamino-17-demethoxy-geldanamycin (17DMAG) and 17-allylamino-17-demethoxygeldanamycin (17AAG) in vitro: effects on Hsp90 and client proteins in melanoma models. *Cancer Chemother Pharmacol* **56:**126–137.

Tian ZQ, Liu Y, Zhang D, Wang Z, Dong SD, Carreras CW, Zhou Y, Rastelli G, Santi DV, and Myles DC (2004) Synthesis and biological activities of novel 17-aminogeldanamycin derivatives. *Bioorg Med Chem* **12:**5317–5329.

Tong W, Cao X, Harris S, Sun H, Fang H, Fuscoe J, Harris A, Hong H, Xie Q, Perkins R, et al. (2003) ArrayTrack—supporting toxicogenomic research at the U.S. Food and Drug Administration National Center for Toxicological Research. *Environ Health Perspect* **111:**1819–1826.

Uehara Y (2003) Natural product origins of Hsp90 inhibitors. *Curr Cancer Drug Targets* **3:**325–330.

Venkateswaran A, Laffitte BA, Joseph SB, Mak PA, Wilpitz DC, Edwards PA, and Tontonoz P (2000) Control of cellular cholesterol efflux by the nuclear oxysterol receptor LXR alpha. *Proc Natl Acad Sci U S A* **97:**12097–12102.

Verrey F, Closs EI, Wagner CA, Palacin M, Endou H, and Kanai Y (2004) CATs and HATs: the SLC7 family of amino acid transporters. *Pflugers Arch* **447:**532–542.

Wang H, Tamba M, Kimata M, Sakamoto K, Bannai S, and Sato H (2003) Expression of the activity of cystine/glutamate exchange transporter, system x_c^-, by xCT and rBAT. *Biochem Biophys Res Commun* **305**:611–618.

Weinstein JN, Myers TG, O'Connor PM, Friend SH, Fornace AJ, Jr., Kohn KW, Fojo T, Bates SE, Rubinstein LV, et al. (1997) An information-intensive approach to the molecular pharmacology of cancer. *Science* **275:**343–349.

Whitesell L, Mimnaugh EG, De Costa B, Myers CE, and Neckers LM (1994) Inhibition of heat shock protein HSP90-pp60v-src heteroprotein complex formation by benzoquinone ansamycins: essential role for stress proteins in oncogenic transformation. *Proc Natl Acad Sci U S A* **91:**8324–8328.

Workman P (2004) Altered states: selectively drugging the Hsp90 cancer chaperone. *Trends Mol Med* **10:**47–51.

Wu G, Fang YZ, Yang S, Lupton JR, and Turner ND (2004) Glutathione metabolism and its implications for health. *J Nutr* **134:**489–492.

Yang P, Ebbert JO, Sun Z, and Weinshilboum RM (2006) Role of the glutathione metabolic pathway in lung cancer treatment and prognosis: a review. *J Clin Oncol* **24:**1761–1769.

Address correspondence to: Ying Huang, Department of Pharmaceutical Sciences, College of Pharmacy, Western University of Health Sciences, Pomona, CA 91766. E-mail: yhuang@westernu.edu